

Dual-band pixelless upconversion imaging devices

Le Ke Wu,¹ Hui Lian Hao,¹ Wen Zhong Shen,^{1,*} Gamini Ariyawansa,² A. G. Unil Perera,² and Steven G. Matsik³

¹Department of Physics, Laboratory of Condensed Matter Spectroscopy and Opto-Electronic Physics, Shanghai Jiao Tong University, 1954 Hua Shan Road, Shanghai 200030, China

²Department of Physics and Astronomy, Georgia State University, Atlanta, Georgia 30303, USA

³NDP Optronics, Mableton, Georgia 30126, USA

*Corresponding author: wzshen@sjtu.edu.cn

Received May 10, 2007; revised June 22, 2007; accepted June 22, 2007;
posted June 26, 2007 (Doc. ID 82883); published August 2, 2007

We have proposed a type of mid-infrared (MIR) and far-infrared (FIR) dual-band imaging device, which employs the photon frequency upconversion concept in a GaN/AlGaN MIR and FIR dual-band detector integrated with a GaN/AlGaN violet light emitting diode. On the basis of the photoresponse of single-period GaN/AlGaN dual-band detectors, we present the detailed optimization of multiperiod GaN emitter/AlGaN barrier detectors and their applications to dual-band pixelless upconversion imaging. Satisfying images have been received through the analysis of the modulation transfer function and the upconversion efficiency in the GaN/AlGaN dual-band pixelless upconverters, which exhibit good image resolution, high quantum efficiency, and negligible cross talk. © 2007 Optical Society of America
OCIS codes: 100.2960, 110.2970, 040.3060.

Beyond the response range (up to $\sim 1 \mu\text{m}$) of the high performance and low cost Si charge coupled devices (CCDs), the imaging of mid-infrared (MIR) and far-infrared (FIR) radiation has a lot of applications. Currently, MIR imaging is often achieved by expensive InSb and HgCdTe arrays, while there are no semiconductor image sensors commercially available for FIR radiation. The concept of photon frequency upconversion [1] provides the possibility for converting arbitrary IR radiation into short wavelength light that falls into the efficient imaging range of conventional Si CCDs. Liu *et al.* [2] have successfully demonstrated MIR detection imaging with an upconverter consisting of a GaAs/AlGaAs quantum well infrared photodetector (QWIP) and an InGaAs/GaAs near-infrared (NIR) light emitting diode (LED). We have proposed a FIR semiconductor upconversion device [3] integrating a GaAs homojunction interfacial work-function internal photoemission (HIWIP) FIR detector [4] with a GaAs/AlGaAs NIR LED. Due to the reduction of the photodetector resistance upon MIR/FIR radiation, the increase of the potential drop across the LED drives the short wavelength emission to be imaged by the Si CCDs. With a sufficient number of periodic structures in QWIPs and HIWIPs, the nonuniformity of the incoming IR light can be almost maintained in the detector photocurrent, and therefore this kind of semiconductor upconversion imaging device is not necessarily separated into pixels [3].

The recent rapid progress in multiband IR detectors establishes an experimental basis for further multicolor operation of the upconversion technology. Dual-band upconversion of MIR radiation at 5 and 9 μm has been reported through the combination of *n*- and *p*-type QWIPs with an LED, which facilitates the realization of sequential multicolor MIR imaging [5]. Very recently, we demonstrated high performance GaN/AlGaN heterojunction IWIP (HEIWIP) MIR and FIR dual-band detectors on sapphire substrates [6]. The main structure of the dual-band detector consists of the single-period Si-doped n^+ -GaN emitter

($5 \times 10^{18} \text{ cm}^{-3}$, 200 nm) and intrinsic $\text{Al}_x\text{Ga}_{1-x}\text{N}$ barrier ($x=0.026$, 600 nm) layers. We will show in this Letter the possibility of implementing MIR/FIR dual-band upconversion imaging.

We start with the response of the single-period GaN/AlGaN dual-band detector. In the MIR range, the photon absorption is due to the free carrier absorption in the GaN emitter layer, followed by the internal photoemission of photoexcited carriers across the work function at the interfacial barrier due to the band offset of GaN and AlGaN, and the photoexcited carriers are collected by the image force to generate photocurrent [6]. Employing the transfer matrix method, we can calculate the MIR light absorption and transmission by introducing the complex dielectric functions of GaN and AlGaN according to the Drude model [7]. The internal photoemission process can be described by an escape cone model [8], and the collection efficiency takes the form in [4]. The theoretical results in Fig. 1(a) can well reproduce the experimental data, clearly demonstrating the free car-

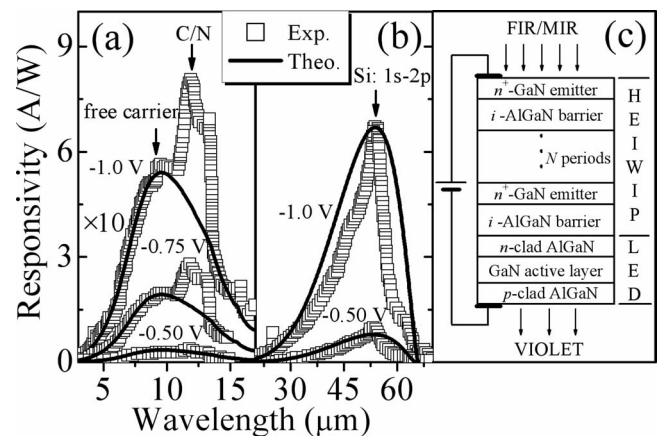


Fig. 1. Spectral response of the single-period GaN/AlGaN dual-band detector at 5.3 K in (a) MIR and (b) FIR ranges, together with (c) the schematic view of dual-band upconverter consisting of a multiband GaN/AlGaN HEIWIP and a normal GaN/AlGaN violet LED.

rier absorption nature of the 8–14 μm response. The strong structures at $\sim 12 \mu\text{m}$ might be due to the unintentionally introduced carbon impurities or nitrogen vacancies in the GaN emitter layer [6], which is excluded from our theoretical considerations.

While in the FIR range, photon absorption is attributed to the shallow donor Si impurity-related $1s-2p$ transition [6]; the electrons excited to the conduction bands are collected by the electric field to contribute to the conductivity, just like in the case of extrinsic photodetectors. We employ the effective-mass approximation theory and the hydrogenic donor model to describe the ionized Si impurity-related $1s-2p$ transition. Combining the absorption efficiency with the collection efficiency, we have displayed in Fig. 1(b) the calculated FIR spectral response. It is clear that the responsivity decreases rapidly away from the FIR absorption center at $\sim 54 \mu\text{m}$, which is the typical characteristic of impurity absorption in semiconductors.

We note that in the single-period GaN/AlGaIn dual-band detector, the MIR photoresponse is comparable with that of multiperiod GaAs/AlGaAs QWIP [9] and HEIWIP [10] detectors, while the FIR one is larger than that of multiperiod GaAs HIWIP detectors [4]. However, the peak absorption efficiency for MIR and FIR in the single GaN emitter layer is only $\sim 20\%$, leaving much room for improvement. We have further calculated the MIR (at $8 \mu\text{m}$) and FIR (at $54 \mu\text{m}$) absorption efficiency in the dual-band detectors with different periods N of GaN emitter/AlGaIn barrier layers [see the HEIWIP part in Fig. 1(c)]. From Fig. 2(a), it is obvious that the absorption efficiency increases rapidly with N , and saturates when N approaches large values. Under large N s, the absorption efficiency for $8 \mu\text{m}$ could be as high as $>90\%$, and that for $54 \mu\text{m}$ can be close to 50% (due to the $\sim 50\%$ FIR reflectivity in the present structures). However, the maximum period should be limited by the impact ionization process and the loss due to scattering and trapping centers in detectors. The relationship between N and the device parameters is given by $2^{N-2}q^2D \leq \epsilon_0\Delta A$ [4], where q is the unit

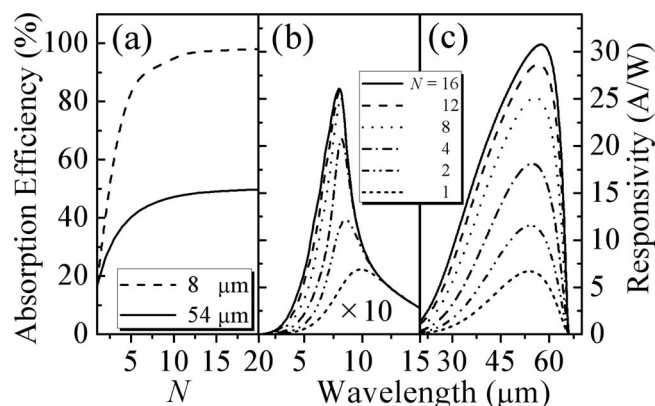


Fig. 2. (a) Absorption efficiency as a function of period number N in GaN/AlGaIn dual-band detectors at 8 and $54 \mu\text{m}$. Calculated spectral response of the dual-band detectors under different period number N in (b) MIR and (c) FIR regions.

charge, D is the thickness of the barrier layer, ϵ_0 is the dielectric constant of vacuum, Δ is the ionization barrier ($\sim 31 \text{ meV}$), and A is the optical window area. Theoretical estimation with these parameters yields $N \leq 16$ as a limit.

We have also calculated the photoresponse of the multiperiod GaN/AlGaIn dual-band detectors in MIR [Fig. 2(b)] and FIR [Fig. 2(c)] ranges. It is expected that the responsivity increases rapidly with N in two wavelength regions, together with the slight blueshift of the peak position (from ~ 9 to $8 \mu\text{m}$) for the MIR photoresponse, and redshift (from ~ 54 to $57 \mu\text{m}$) for the FIR one. For the application of pixelless upconversion imaging devices, a multiperiod structure is an important requirement for the IR detector, where the output distribution of the photocurrent density driving the LED can well reproduce the spatial distribution of the incident IR radiation intensity, and the semiconductor upconverter is not necessarily separated into pixels [3]. The significant enhancement of the responsivity in multiperiod dual-band detectors, as compared with that in single-period counterparts, indicates that the multiperiod GaN/AlGaIn detector could serve as a good candidate for the dual-band pixelless upconversion imaging device. As for the responsivity peak shift, skin depth and cavity effects [10] are the two main factors.

The MIR and FIR dual-band upconversion imaging can be achieved by integrating the GaN/AlGaIn dual-band detector with a compatible normal GaN/AlGaIn violet LED. Figure 1(c) presents the schematic structure of the proposed dual-band upconverter. We analyze the performance of the dual-band upconverter using the spectral decomposition approach. The current continuity equation in the detector [3] as well as the carrier diffusion equation in the LED [8] with the photon recycling effect [11] can be solved to obtain the modulation transfer function (MTF) and the quantum efficiency of the upconverter. Figure 3 presents the spatial frequency f dependences of the MTF

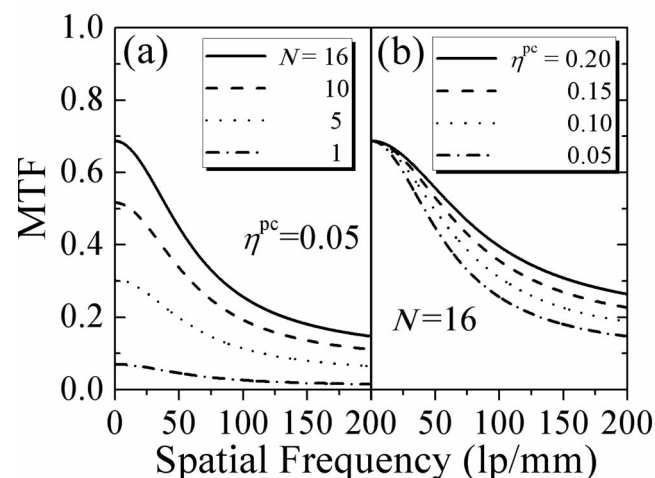


Fig. 3. Spatial frequency dependence of the modulation transfer function (MTF) at various (a) period number N of the dual-band detectors under the LED extraction efficiency $\eta^{\text{pc}}=0.05$, and (b) η^{pc} of the violet LEDs under $N=16$.

under various N of the GaN/AlGaIn dual-band detector [Fig. 3(a)] and photon extraction efficiency η^{pc} of the GaN/AlGaIn LED [Fig. 3(b)]. The MTF value increases with N , indicating that the multiperiod dual-band detector provides a high contrast transfer capability. Considering the period number limitation discussed earlier, we will select $N=16$ for the dual-band detector to implement the upconversion imaging.

On the other hand, due to the internal total reflection, the extraction efficiency of the photons generated in conventional LEDs is always low, while $\sim 20\%$ of η^{pc} could be achieved in a resonant cavity enhanced LED [8]. With the enhancement of η^{pc} , fewer reincarnation cycles are needed by an average violet photon to escape the LED during the photon recycling process [11], resulting in the reduction of the carrier diffusion in the LED, and therefore the improvement of the image characteristics in Fig. 3(b). Under a high extraction efficiency of 20%, the diffusion of carriers in the LED will be less than the smallest nonuniformity limited by diffraction, which leads to negligible image smearing. As a result, MTF(f)/MTF(0) is always larger than 0.5 in the whole spatial frequency range, indicating that the perceived sharpness and resolution could be obtained even in the size of the details.

The quantum efficiency of the upconverter is also a key parameter for imaging. We have investigated the relationship between the upconversion efficiency and emitter layer thickness under different η^{pc} at two typical wavelengths of 8 and 54 μm , as shown in Fig. 4, where large emitter layer thickness results in high upconversion efficiency. However, when the thickness is greater than the carrier diffusion length (~ 250 nm) in GaN, only a fraction of carriers contributes to the output current density, and the others will lose in the diffusion due to the scattering losses, so the upconversion efficiency tends toward saturation. At the same time, with increasing η^{pc} , the parasitic and nonradiative losses in the photon recycling pro-

cess are small. As a result, the upconversion efficiency is also expected to increase with η^{pc} . It should be noted that, under the present optimal parameters, the quantum efficiency of $\sim 20\%$ in the GaN-based dual-band upconversion imaging device is much higher than that of the GaAs-based QWIP-LED ($\sim 1\text{--}3\%$) MIR and HIWIP-LED ($\sim 1\%$) FIR upconverters [3], showing the excellent performance and potential application.

Finally, we discuss effective ways to separate the response from the two bands and how to avoid the cross-talk phenomenon resulting from the leaked LED violet radiation absorbed by the GaN emitter layer of the detector. Due to the diffraction effect, only images with $f \leq 1/\lambda$ (λ is the wavelength of the incoming IR radiation) could be resolved [3]. The object of the MIR radiation will have a much finer image than that of the FIR one; i.e., we can distinguish the MIR and FIR images though both components would be upconverted to the violet photons. More effective upconversion structures could be designed by introducing voltage switch control [5] or multicontact techniques for the selective upconversion imaging of MIR and FIR radiation. On the other hand, taking advantage of the high reflectivity of the distributed Bragg reflectors (DBRs) [8], we can significantly block the violet photons from reaching the dual-band detector by sandwiching top and bottom DBR mirrors (serving as the resonant cavity) for the GaN/AlGaIn LED, so that the cross talk between the LED and the dual-band detector is negligible.

This work was supported by the Natural Science Foundation of China under contract 60576067, and Shanghai Municipal Commission of Science and Technology Project 05QMH1411, as well as the U.S. Air Force Small Business Innovation Research Program (SBIR) under grant FA9453-05-M-0106.

References

1. P. W. Kruse, F. C. Pribble, and R. G. Schulze, *J. Appl. Phys.* **38**, 1718 (1967).
2. H. C. Liu, J. Li, Z. R. Wasilewski, and M. Buchanan, *Electron. Lett.* **31**, 832 (1995).
3. L. K. Wu and W. Z. Shen, *J. Appl. Phys.* **100**, 044508 (2006).
4. W. Z. Shen, A. G. U. Perera, H. C. Liu, M. Buchanan, and W. J. Schaff, *Appl. Phys. Lett.* **71**, 2677 (1997).
5. E. Dupont, M. Gao, Z. Wasilewski, and H. C. Liu, *Appl. Phys. Lett.* **78**, 2067 (2001).
6. G. Ariyawansa, M. B. M. Rinzan, M. Strassburg, N. Dietz, A. G. U. Perera, S. G. Matsik, A. Asghar, I. T. Ferguson, H. Luo, and H. C. Liu, *Appl. Phys. Lett.* **89**, 141122 (2006).
7. T. Kozawa, T. Kachi, H. Kano, Y. Taga, M. Hashimoto, N. Koide, and K. Manabe, *J. Appl. Phys.* **75**, 1098 (1994).
8. L. K. Wu and W. Z. Shen, *IEEE J. Quantum Electron.* **43**, 411 (2007).
9. B. F. Levine, *J. Appl. Phys.* **74**, R1 (1993).
10. D. G. Esaev, S. G. Matsik, M. B. M. Rinzan, A. G. U. Perera, H. C. Liu, and M. Buchanan, *J. Appl. Phys.* **93**, 1879 (2003).
11. I. Schnitzer, E. Yablonovitch, C. Caneau, and T. J. Gmitter, *Appl. Phys. Lett.* **62**, 131 (1993).

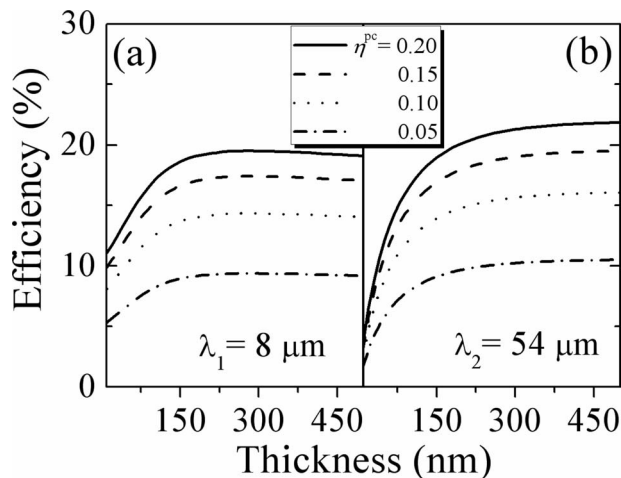


Fig. 4. Calculated upconversion efficiency as a function of GaN emitter layer thickness for the 16-period GaN/AlGaIn dual-band detector at different extraction efficiency η^{pc} of the GaN/AlGaIn violet LEDs, under the incoming wavelength of (a) $\lambda_1=8 \mu\text{m}$ and (b) $\lambda_2=54 \mu\text{m}$.